

Wireline and While-Drilling Formation-Tester Sampling with Oval, Focused, and Conventional Probe Types in the Presence of Water- and Oil-Base Mud-Filtrate Invasion in Deviated Wells

Abdolhamid Hadibeik, The University of Texas at Austin, Mark Proett, Halliburton Energy Services, Carlos Torres-Verdín, Kamy Sepehrnoori, and Renzo Angeles, The University of Texas at Austin

Copyright 2009, held jointly by the Society of Petrophysicists and Well Log Analysts (SPWLA) and the submitting authors.

This paper was prepared for presentation at the SPWLA 50th Annual Logging Symposium held in The Woodlands, Texas, United States, June 21-24, 2009.

ABSTRACT

Speculation about the potential of developing new fluid sampling methods with probe-type formation testers has existed since the introduction of formation pressure testing to the drilling environment in 2002. Extending the existing wireline technology requires a new pumping system capable of removing invasion fluids and then filling single-phase sample chambers. Several technology advances are necessary before this is commercially possible. Although wireline pumpout tools may require hours to retrieve representative fluid samples, spending hours obtaining samples in the drilling environment may not be considered a practical alternative. The objective of this paper is to quantify the viability of sampling in the drilling environment by way of numerical simulations. The study considers the dynamic nature of invasion while drilling when using both new and conventional probe configurations to retrieve fluid samples.

Previous studies assumed a time-constant rate of invasion that was close to that of the final stages of invasion. Furthermore, most simulations of wireline formation-tester measurements assumed that invasion ended at the time when fluid pumpout began. Both of these assumptions are optimistic for a drilling tool. To more realistically simulate the invasion during drilling, a mudcake model is used that continues to grow in thickness and sealing effectiveness during invasion and throughout the sampling process. With this mudcake model there are higher rates of invasion soon after drilling. Simulation results focus on scenarios in which water-base mud (WBM) and oil-base mud (OBM) invade an oil-bearing zone. Also studied are the accuracy of functions used to estimate contamination in an OBM environment. The base model consists of a typical probe-type tool in a vertical well wherein fluid samples are retrieved using a time-constant flow rate. Invasion time is varied from 1 to 48 hours to compare drilling and wireline sampling tools. This study

quantifies mudcake sealing effectiveness, as well as the effect of borehole deviation. Oval (elongated) and focusing guard-style probes are compared to standard probe configurations in various petrophysical rock types.

Simulations of fluid cleanup times for a variety of rock types and wellbore deviation angles indicate that the oval focused probe retrieves the cleanest fluid sample in the least amount of time.

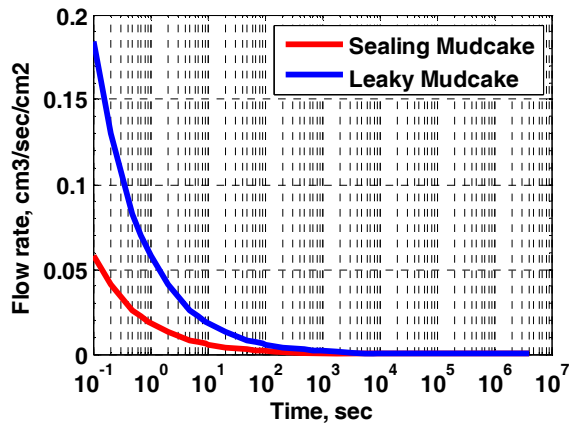
INTRODUCTION

It has long been realized that sampling fluids and measuring pressures in porous rock formations early in the life of a well provides valuable information about the capability of the formation to produce oil and/or gas. Therefore, there is a significant demand for a new generation of formation-testers that can reduce both time of sampling and rig time. Moreover, formation testers are required to secure representative downhole fluid samples, even in complex situations when filtrate is miscible with in-situ reservoir fluid. The industry has introduced optical fluid identification modules for real-time monitoring (Mullins and Schroer, 2000), focused sampling probes (Sherwood, 2005) and, quite recently, the oval pad tester (El Zefzaf et al., 2006). Nonetheless, one of the most important issues with wireline formation sampling remains acquiring clean reservoir fluid samples with a minimum of mud-filtrate contamination as early as possible in the life of the well.

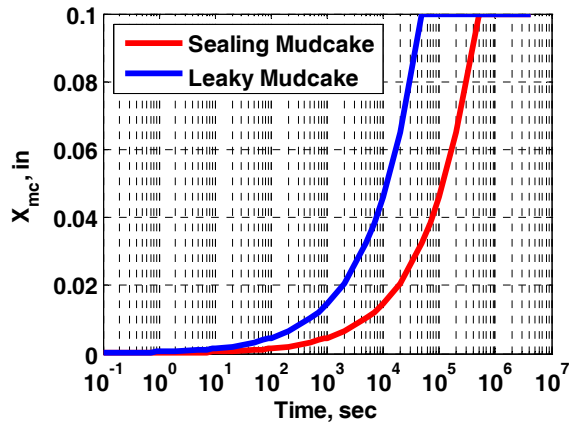
Although wireline testers are mature technology, new while-drilling formation-testers are emerging, but are currently only designed to measure reservoir pressure (Proett et al., 2003). Even though sampling-while-drilling could be implemented in practice, it is not clear to what extent and how comparable fluid samples would be relative to those acquired with wireline formation testers. Similarly, it is not clear what type of formation-tester probe should be used to ensure

minimally contaminated measurements for a specific tool/formation configuration.

Although the effectiveness of fluid sampling in the drilling environment can be simulated, it is important to consider how invasion occurs while drilling. It is, therefore, pertinent to consider current techniques used for simulation of mud-filtrate invasion.



(a) Flow rate of mud-filtrate invasion



(b) Thickness of the mudcake

Fig. 1: Simulation of sealing and leaky mud-filtrate invasion. Flow rate and mudcake thickness vary with time. Filtrate loss is negligible at late times and mudcake thickness becomes constant. Although leaky mudcake builds up faster, it entails more filtrate loss than sealing mudcake.

Previously, simulations of fluid cleanup were initialized with a known volume of mud-filtrate invasion (Malik et al., 2009). Other works simulated mud-filtrate invasion before the onset of fluid pumpout, but then the invasion rate was stopped after pumpout began (Alpak et al., 2008; Angeles et al., 2009). Both methods are optimistic when analyzing logging-while-drilling (LWD) measurements, given that the mudcake is not fully formed at these early stages of drilling and mud-

filtrate invasion continues regardless of the formation test.

The central objective of this paper is to compare while-drilling and wireline testers to quantify their effectiveness under different fluid conditions, various petrophysical rock types, and different wellbore deviation angles. These comparisons include the simulation results of recently introduced formation-tester probe geometry that is intended to achieve faster cleanup times with lower pressure drops imposed on the formation.

To explicitly incorporate the effects of mud-filtrate invasion before and during formation testing, a 3D multi-phase, multi-component reservoir simulator is used that considers gravity and capillary pressure. Mud-filtrate invasion is simulated using a modification of the method proposed by Wu et al. (2004). Subsequently, the effects of various contamination functions are investigated to evaluate the assessment of fluid sample quality with time of sampling.

It is also necessary to elaborate on the definition of contamination, which is critical when filtrate is miscible with reservoir fluid. Previous studies proposed to measure gas-oil ratio (GOR) to distinguish the level of contamination of a fluid sample (Alpak et al., 2008). This study indicates considerable differences in the assessment of cleanup time when other types of physical measurements are used to estimate levels of fluid contamination (e.g., viscosity and density of mud filtrate). These methods are evaluated to assess contamination against simulations in which contamination is known *a priori*. In addition, numerical simulations consider the effect of borehole deviation on the performance of various probe configurations.

NUMERICAL SIMULATION

The cases described in this paper use a multi-phase, multi-component reservoir simulator supported by CMG¹. However, the same method can be applied to other numerical reservoir simulators. In the case of WBM filtrate invasion, simulations are performed with a black-oil reservoir method. In this model, capillary pressure, relative permeability, and other rock-fluid properties, which depend on fluid saturation, are included in the simulations, and the model accounts for the effect of gravity. For simplicity, there is no difference between imbibition and drainage capillary pressure and relative permeability curves during the process of mud invasion and the pumpout sampling stage. A compositional Equation-Of-State (EOS)

¹ CMG: Computer Modeling Group Ltd.

simulator is used for OBM filtrate invasion and sampling.

To make these simulations more accurate, particularly for the FTWD, mud invasion must continue during the drawdown or pumpout stages of the simulation. However, mud invasion is prevented from flowing in a selected area of the probe defined as where the probe creates a seal against the wellbore. Mud invasion continues until the end of the buildup test. However, the invasion rate can vary throughout the entire process and depends on the dynamic filtration mudcake model described in the next section. As shown in **Fig. 1**, most filtrate loss typically occurs soon after drilling through the rock and is frequently referred to as the spurt or surge loss.

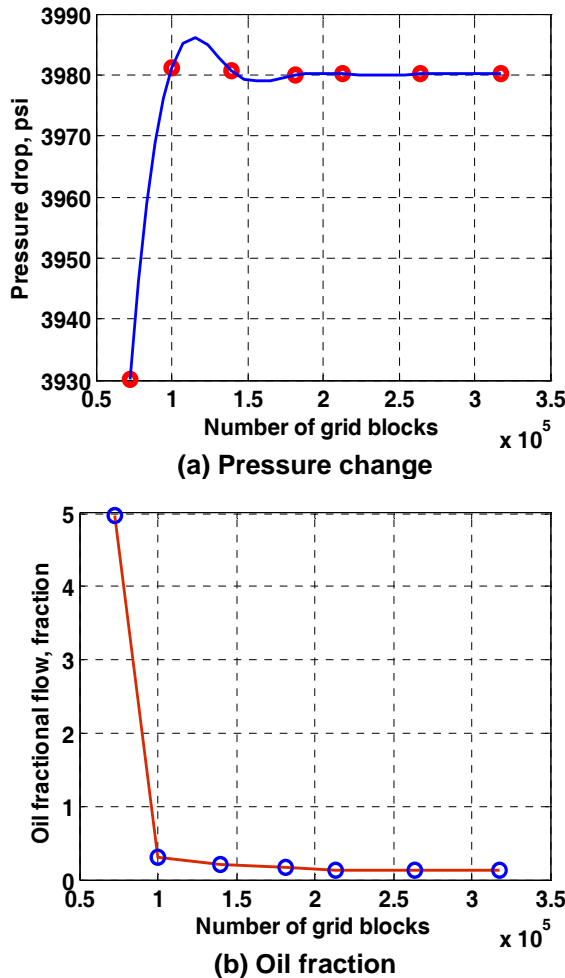


Fig. 2: Grid refinement study to appraise simulations of fractional flow and pressure drop measurements. The number of grid blocks increases until simulation results no longer depend on the number of grid blocks. Comparisons are made using simulations of pressure drop both at the start of fluid pumpout and at the time when the probe reaches 5 % of clean oil.

The wellbore boundary is defined by a fine mesh of square grid blocks in the simulation model. Grid blocks adjacent to the wellbore use no flow boundary condition; however, mud invasion is simulated by including injection point sources on the grid blocks surrounding wellbore. This strategy also enables the simulation of invasion-sampling test cases in deviated and horizontal wells.

The type of probe used and its overall dimensions determine how the fundamental base grid blocks are defined. Matching the probe to the simulation grid is a critical step in the modeling because modeling errors can occur in this region as a result of high pressure and fluid-concentration gradients. The goal is to size the grid blocks so that the number and size of grid blocks result in convergence of the solution. Ideally, when a grid is refined and the solution converges, small variations in the gridding will not affect the result of numerical simulation. **Fig. 2** shows the numerical study for the oval and oval focused probe. Grid refinement continues until the effect of numerical error attributable to discretization is minimized.

DYNAMIC MUDCAKE MODELING

The process of modeling dynamic mud-filtrate invasion was first described by Chin (1995), and later used by Wu et al. (2004) to numerically simulate mud-filtrate invasion in deviated wells. This mudcake model was originally developed from first principles by considering the filtration of a fluid suspension of solid particles by a porous but rigid mudcake. It can also be shown that this fundamental model couples mudcake growth to mudcake properties, formation properties as well as dynamic conditions in annular pressure. A simplified form of the mudcake growth model is given by

$$x_{mc}(t) = \frac{1}{2.54} \sqrt{\frac{2t\Delta P\lambda k_{mc}}{14,696 \mu_m}}, \quad (1)$$

where x_{mc} is mudcake thickness (in.), t is time of invasion (sec), k_{mc} is mudcake permeability (mD), ΔP is pressure drop across the mudcake (psi), μ_m is mud viscosity (cp), and λ is growth factor. As shown in Eq. 1, mudcake thickness depends on the pressure drop across the sandface, and pressure drop depends on the flow rate of mud invasion, which is a function of mud thickness. Flow rate of mud invasion is obtained from

$$q(t) = \frac{2.54 k_{mc} \Delta P}{14,696 \mu_m x_{mc}(t)}, \quad (2)$$

where $q(t)$ is mud invasion flow rate ($\text{cm}^3/\text{sec}/\text{cm}^2$). The filtrate viscosity, mudcake permeability, and growth

factor are assumed to remain constant during the invasion process. Flow rate and growth thickness of mudcake are determined in an iterative loop combined with the CMG simulator. Another significant difference in this work is that mud-filtrate invasion continues during the pumping or sampling phase. For this reason, samples will never reach 0% contamination, as is the case in practical conditions.

In the simulation of WBM and OBM filtrate invasion, both drilling fluids have the same radial length of invasion, time of invasion, and flow rate of invasion. Simulations indicate that, as a result of capillary effect, WBM spreads more than OBM in the radial distance, and that OBM results in more a piston-like radial front of invasion.

TABLE 1: Summary of assumed mudcake properties

Variable	Units	Value
Maximum Thickness	in	0.1
Overbalance Pressure	psi	1000
Filtrate Viscosity	cp	1
Mudcake perm.	mD	0.0001* 0.001**
Growth Factor	-	0.01

*Sealing mudcake, **Leaky mudcake

TABLE 2: Summary of petrophysical properties assumed for different rock types

Rock Type	k (mD)	Anisotropy	ϕ	S_{wirr}
1	1	1	0.1	0.21
2	10	0.1	0.16	0.16
3	100	0.1	0.2	0.11
4	500	1	0.3	0.07

Fig. 1 shows the calculated flow rate and thickness of the mudcake. The result is in agreement with the experiment that Fisk and Jamison (1989) report in their work. The amount of filtrate loss varies with borehole deviation angle. An increase in wellbore deviation angle increases the volume of mud invasion. Combining the dynamic mudcake modeling directly in the simulation, makes it possible to model the difference between while-drilling and wireline formation-testers. Results would be optimistic if the mud invasion flow rate were considered to be time-constant throughout the simulation, or if the mud-filtrate invasion were stopped during the pumpout test. **Table 1** summarizes the properties of the sealing and leaky mudcake used in this paper.

The filtrate loss also depends on the rock type and varies with the permeability and porosity of the

reservoir. In turn, the radius of mud invasion also depends on changes in the permeability and porosity of the rock.

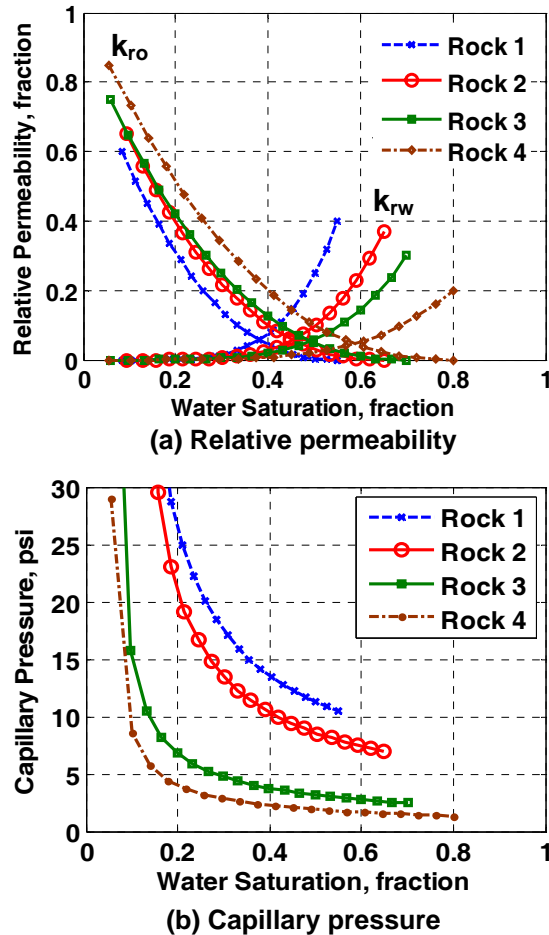


Fig. 3: Saturation-dependent, relative permeability, and capillary pressure for four synthetic oil-wet rock types (k_{ro} and k_{rw} are oil and water relative permeability, respectively). As permeability and porosity decrease, relative permeability to oil decreases and capillary pressure increases.

VALIDATION

Fig. 2 shows results from grid refinement studies for the model of oval and oval focused probe. For single and focused-sampling probes, the grid mapping used closely matches that used by Angeles et al. (2009). This has the advantage of using an established grid in which validations for the numerical discretization and convergence have been established. For the new oval and oval focused probes, the size of grid blocks must conform to the size of the probe geometry, making it necessary to validate the new gridding strategy. As a result, a base-case model was defined with 317,580 finite-difference grids that constrained the maximum

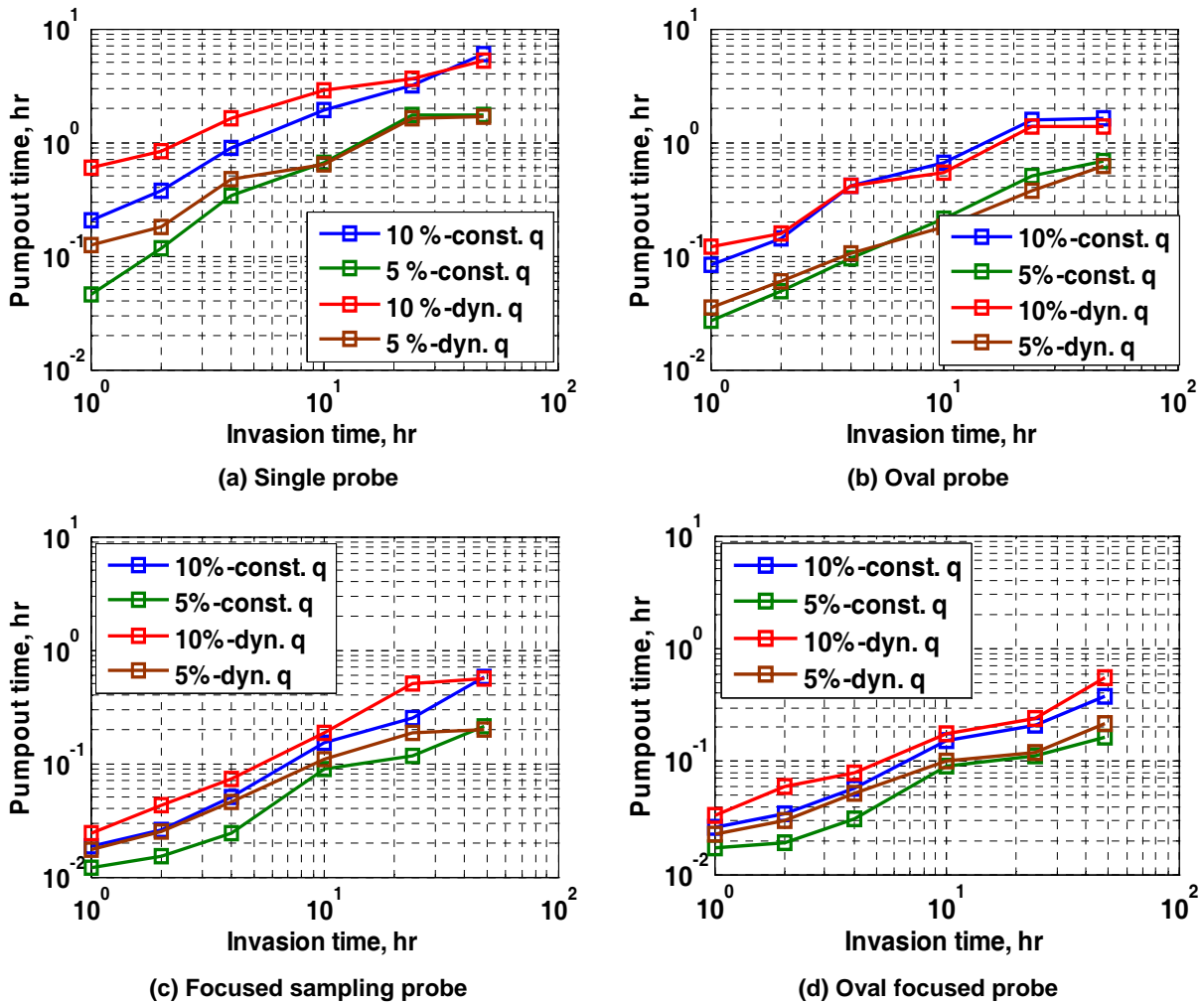


Fig. 4: Comparison of dynamic mud flow rate, and constant-rate mud-filtrate invasion with sealing mudcake for 10% and 5% of contamination. At short invasion times, the constant-rate invasion model is optimistic, and indicates faster fluid cleanup than dynamic mud-filtrate flow rate. At long high invasion times, the difference between the two becomes smaller than at short invasion times.

error bounds to less than 0.05% for the simulated fractional flow rate and pressure.

PETROPHYSICAL ASSUMPTION

In this paper, the base-case model is assumed to be an anisotropic homogenous reservoir. The same capillary pressure and relative permeability curves are used for drainage and imbibition. This simplification was made because previous work showed that such an assumption normally causes very small differences in the simulated pumpout times. **Table 2** summarizes the rock properties, and **Fig. 3** shows the relative permeability and capillary pressure curves used in the simulations. Rock Type 3, in Table 2, is the base-case model. The synthetic rock types include a wide range of petrophysical properties of reservoirs and are used to

evaluate the cleanup time in each case of wireline and while-drilling formation-testers.

TYPES OF FORMATION-TESTER PROBE

Four types of probes are used in the analysis, including a single probe or conventional probe, an oval pad or elongated oval shape probe, a focused sampling probe, and an oval focused probe. **Fig. 5** shows the configuration of the last two probes in the simulation.

The focused sampling probe and the oval focused probe include two types of probes or flow areas: the sample probe and a guard ring that surrounds the inner sample probe. Although a sample probe acquires the fluid sample, a guard ring withdraws the contamination surrounding the probe.

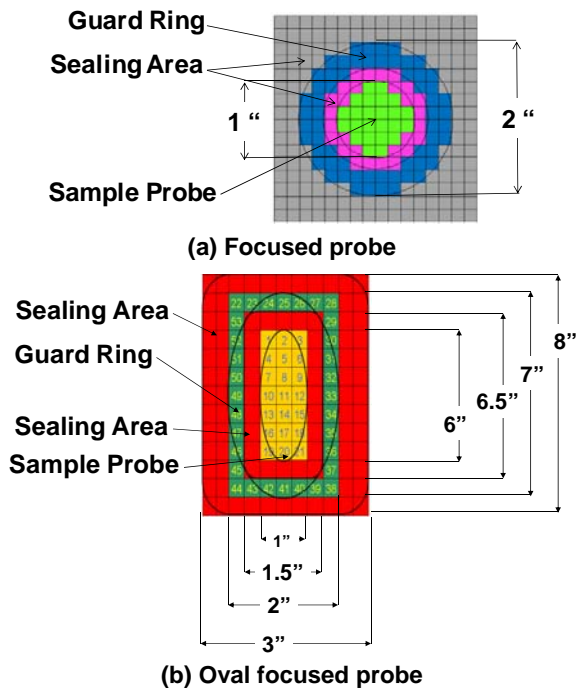


Fig. 5: Spatial discretization of (a) focused sampling, and (b) oval focused probe. Sample probe and guard ring for each probe are defined with point sources within in each grid block. Mud-filtrate invasion stops at probe locations during fluid pumpout.

MODELING RESULTS

WBM

In the WBM case, a black-oil reservoir simulator is used with the mud-filtrate invasion time varying from 1 to 48 hr, which includes the framework ranging from while-drilling to wireline formation-testers. **Table 3** and **Table 4** summarize the reservoir and fluid properties used. When pumpout starts, fluid from the reservoir begins to flow into the probe, and mud invasion continues into the formation except for the sealing area of the probes. The cleanup time is calculated from the beginning of the pumpout. Fractional flow of water to oil entering the probe represents the contamination function for WBM. Two cleanup times are recorded when the contamination level reached 5% and 10% respectively (see **Fig. 6**).

Fig. 4 shows the difference between constant-rate mud-filtrate invasion and dynamic mud-filtrate invasion for the four types of probes. For the constant-rate mud invasion case, the rate is determined by averaging the rates for the dynamic mud-filtrate during the mud invasion period. When comparing the same probe design, the difference between the time-constant invasion rate case and dynamic invasion case is negligible at long invasion times (i.e., greater than 24

hours). Such a situation arises because mudcake is completely formed for the dynamic case and the total filtrate loss is similar to the constant invasion case. These simulation results are obtained using the sealing mudcake properties; results will vary with the mudcake properties used.

TABLE 3: Summary of assumed reservoir properties

Property	Units	Value
Wellbore Radius	ft	0.354
External Radius	ft	160.0
Reservoir Thickness	ft	30.0
Rock Compressibility	1/psi	3.0e-10

TABLE 4: Summary of assumed fluid properties for the WBM case

Property	Unit	Value
Oil Density	lbm/ft ³	52.4
Water Density	lbm/ft ³	62.4
Oil Compressibility	1/psi	3.0e-6
Water Compressibility	1/psi	2.5e-6
Oil Viscosity	cp	0.5
Water Viscosity	cp	1.0
Oil Bubble Point Press.	psi	500

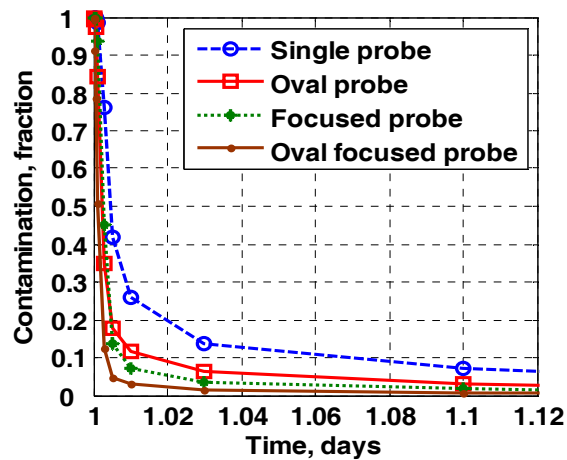


Fig. 6: Contamination function associated with four-probe type formation testers for the base-case model. Drawdown begins after 24 hours of WBM invasion. Contamination at the probe is measured as a function of time.

PROBE COMPARISON

When comparing probe types, it is necessary to use a flow rate that is realistic in practical field conditions. The pumpout flow rate of each probe type depends upon several factors:

- Probe geometry,
- Available pumping capacity (i.e., pressure vs. rate),

- Reservoir and fluid properties, particularly when it is necessary to maintain the pressure drop to maintain single-phase flow when sampling.

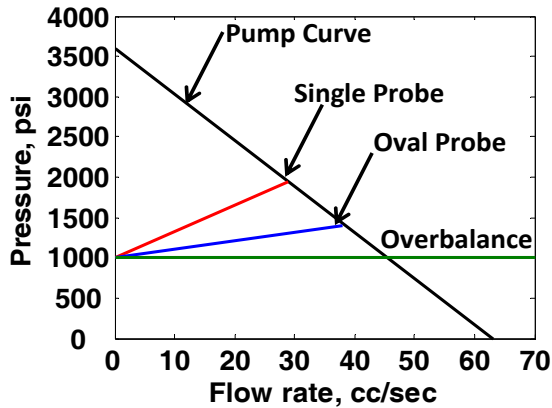


Fig. 7: Idealized pump performance curve and comparison between single and oval probe performance for the base-case model with a 100 mD/cp formation. Drawdown flow rate of probes and the resulting pressure drop should both be chosen below the pump curve to consider the operational safety margin for the pump.

For the pumping capacity, the idealized linear pumping curve shown in **Fig. 7** was considered. Because the pump must first overcome the overbalance before it can move reservoir fluid, the pump capacity is reduced, as shown in **Fig. 7**. Then the probe geometry, rock type, and fluid properties can be used to generate an idealized linear curve for each probe, similar to that shown in **Fig. 7** for the single probe and oval probe (El Zefzaf et al., 2006). Therefore, it is possible to pump at a rate below and up to where the probe curve intersects the pump curve. Because the focused sampling probe and single probe have an equivalent shape and flow area, their pumpout flow rates and pressures are nearly the same. However, as a result of the larger opening of the oval and focused oval probes, they enable greater flow rates than a simple probe at lower pressure differentials in the same conditions (i.e., same pump, rock, and fluid types). While in practical field conditions, these curves may not be linear and can shift during pumpout when fluid fractions change, the relative flow rate differences between the two probe types remain the same.

Fig. 7 shows that for the oval probe, a rate of up to 38 cc/sec is possible. However, to maintain control during pumping, a lower rate is used to remain within the operating margins of the pump. In the base case simulations, a rate of 30 cc/sec is chosen for the oval and focused oval probes. For the single and focused probes to maintain the same differential pressure during pumpout, a rate of 10 cc/sec is used. This normalizes the flow rates for each probe such that the pressure drop would be nearly the same during pumpout for all probe types.

The pumpout flow rate of the focused probe and the oval focused probe are divided into two flow rates: one for the sample probe and one for the guard ring. The respective flow rate of the sample probe to the guard ring can be determined by observing the ratio of the rates between the sample and guard ring, which maintains approximately the sample pressure drop for both regions. As a result, the guard rings have a faster flow rate than the sample inner probes. To keep the relative flow rates normalized between the different probe types, the total flow rate for the focusing probes is equal to the rates used for the unfocused versions. **Table 5** shows the pumpout flow rate for each probe in the base-case model reservoir. Although the drawdown flow rate of the probes changes across the various rock types, the same analysis is applied to obtain the pumpout flow rates for each probe.

TABLE 5: Pumpout flow rate of different probes in base-case model

Probe Type	Pumpout flow rate
Single probe	10.0 (cc/sec)
Oval probe	30.0 (cc/sec)
Focused sampling probe	2.5 (cc/sec) Sample probe 7.5 (cc/sec) Guard ring
Oval focused probe	15 (cc/sec) Sample probe 15 (cc/sec) Guard ring

Fig. 8 indicates the pressure drop of the oval focused probe and focused sampling probe by deviation angles. The use of the oval type probe decreases the pressure drop, especially in highly deviated and horizontal wells.

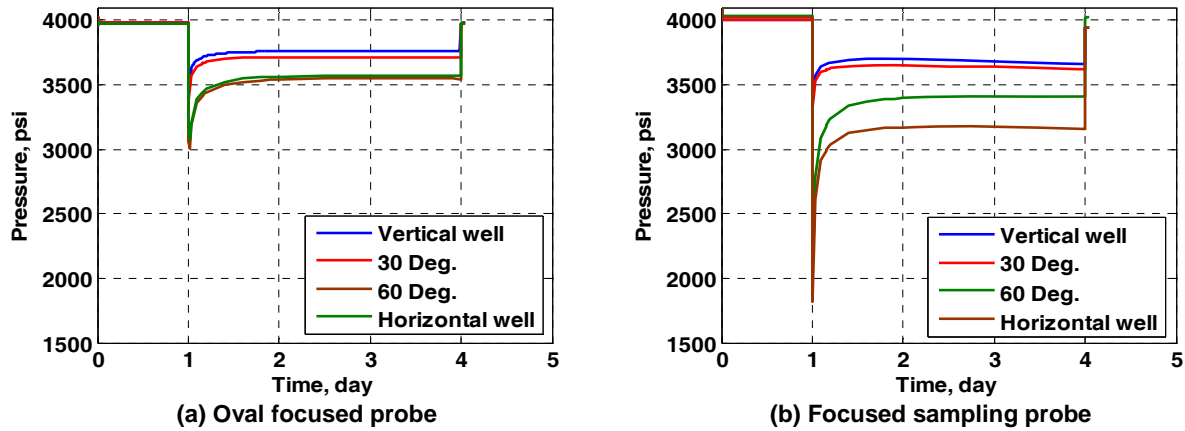


Fig. 8: Pressure drop for (a) oval focused probe and (b) focused sampling probe. The pumpout test begins and the transient pressure drop is recorded after 1 day of mud-filtrate invasion. Increasing the wellbore deviation angle increases the pressure drop during drawdown for each type of probe.

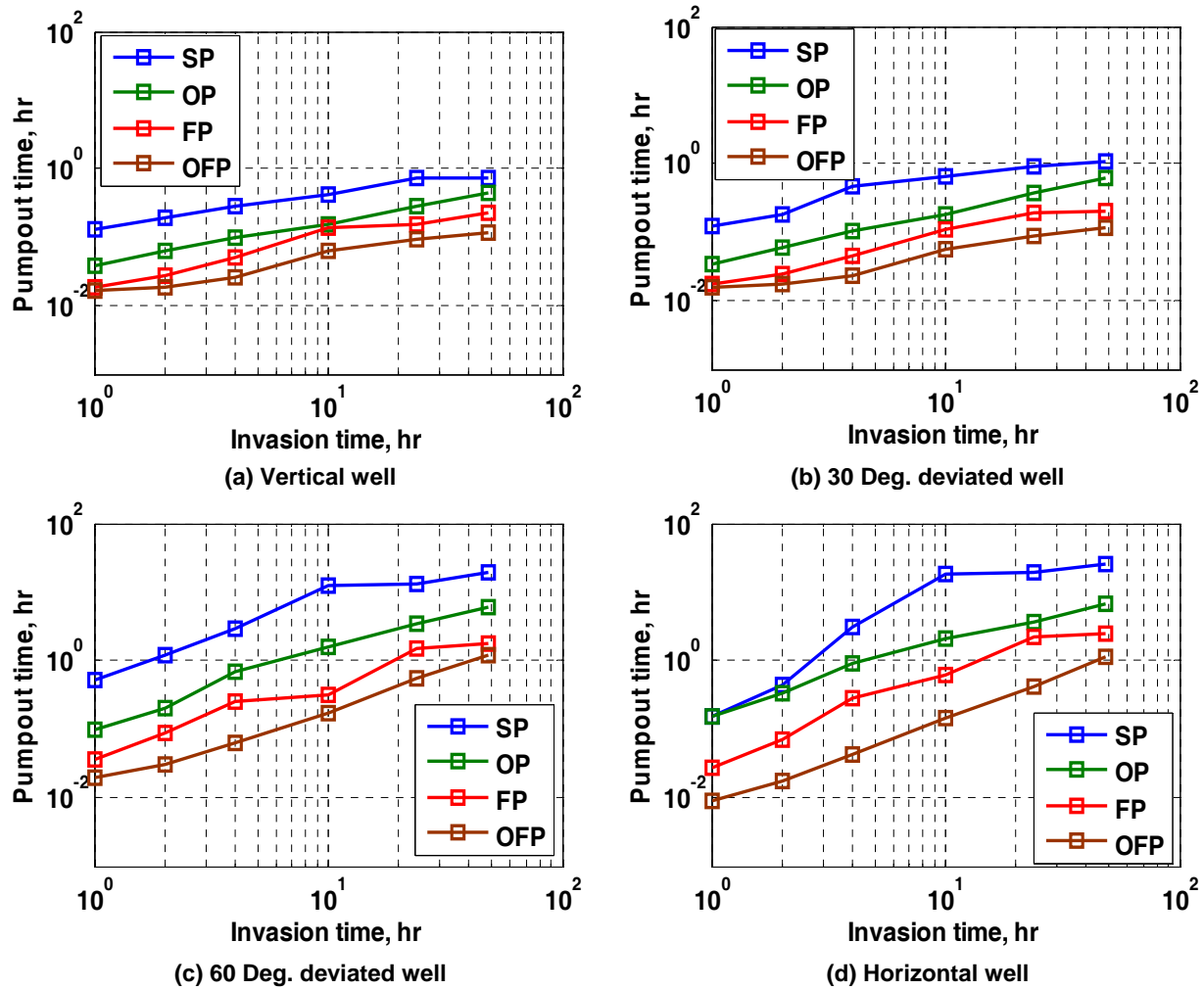


Fig. 9: Pumpout time for cleanup in WBM invasion and type of probe in base-case model (OFP: oval focused probe, FP: focused sampling probe, OP: oval probe, SP: single probe). The time in which each probe reaches to 10 % of contamination is measured. While-drilling formation-testers work in low invasion time, and wireline formation-testers work in large invasion time. The pumpout time required to obtain a clean sample for wireline formation-testers is larger than while-drilling formation-testers.

The pumpout time required to reach 10% contamination is used to compare the probes in Fig. 9. The four plots show simulations in a vertical well, a 30 degree deviated well, a 60 degree deviated well, and a horizontal well. As shown, increasing the deviation angle increases the pumpout time for all probe types. Each plot also shows that increasing the invasion time increases the pumpout time. This observation indicates that while-drilling formation-testers can obtain a 10% contaminated sample much faster than a wireline tool. Another important observation for wireline formation-testers is that they are more affected by the deviation of the wellbore than while-drilling formation-testers, which work within shorter invasion times. Fig. 9 also illustrates that the probes are consistently ordered in pumpout time from the single, oval, focused, and the oval focused probe which has the shortest pumpout time. Furthermore, this order is maintained in all base case simulations when the invasion time and wellbore deviation are varied.

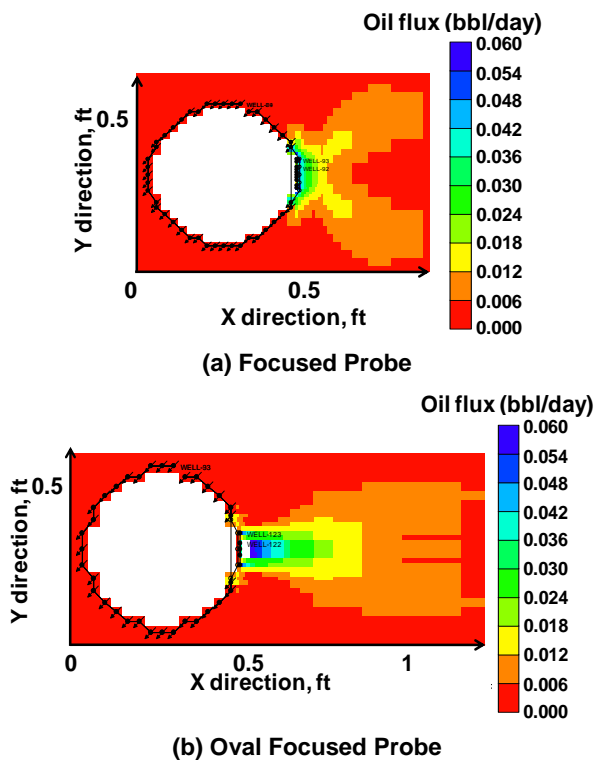
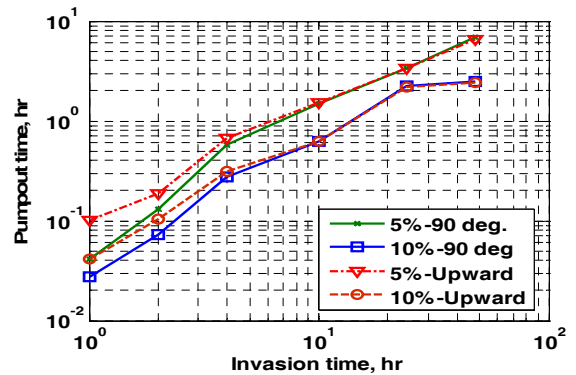


Fig. 10: Oil flux magnitude at the probe during fluid pumpout. Horizontal slices at the borehole illustrate the difference between oil-flux magnitude for both the focused and the oval focused sampling probe.

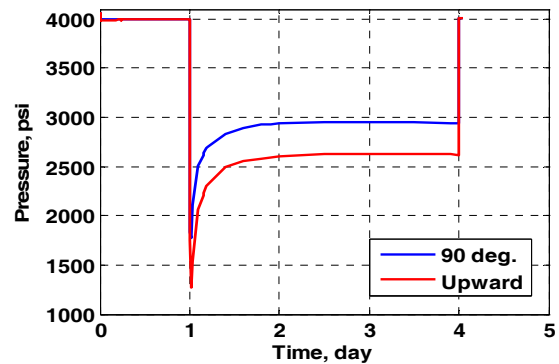
PROBE ORIENTATION

Probe orientation is one of the most important factors affecting the cleanup time. The best location of the probe depends on the anisotropy, heterogeneity, capillary pressure of reservoir, and gravity. Because of

the gravity effect, it is reasonable to assume that orienting the probe on the top sides of the borehole in deviated wells would reduce pumping time. Gravity tends to drain the invading fluid from the top side of the wellbore and decrease the volume of contamination to be removed (Angeles et al., 2009). However, the studies described in this paper indicate that, in the case of a horizontal well and in the presence of anisotropy, (i.e., when horizontal permeability is higher than vertical permeability), the probe should face the upper side of the wellbore (i.e., 90 degree rotation from the top of the wellbore; see Fig. 11).



(a) Sample cleanup time vs. probe orientation



(b) Pressure drop vs. probe orientation

Fig. 11: Comparison of probe locations along the perimeter of a horizontal wellbore. When the probe is located on the side of the well (90 degree orientation from top of the wellbore), cleanup time is faster for short invasion times than when the probe is located at the top of the wellbore (upward position). For the case of pressure drop, there is a lower pressure drop during fluid pumpout when the probe is located to the side of the well. Simulation results were obtained for the base-case model and rock type no. 3, assuming a horizontal/vertical permeability ratio of 10:1.

Probe orientation becomes more critical in the case of low invasion times encountered with while-drilling formation-testers than in the case of wireline testers. For longer invasion times, the difference in pumpout time with the various probe orientations is not as large. Fig. 11 also illustrates that when the probe faces the

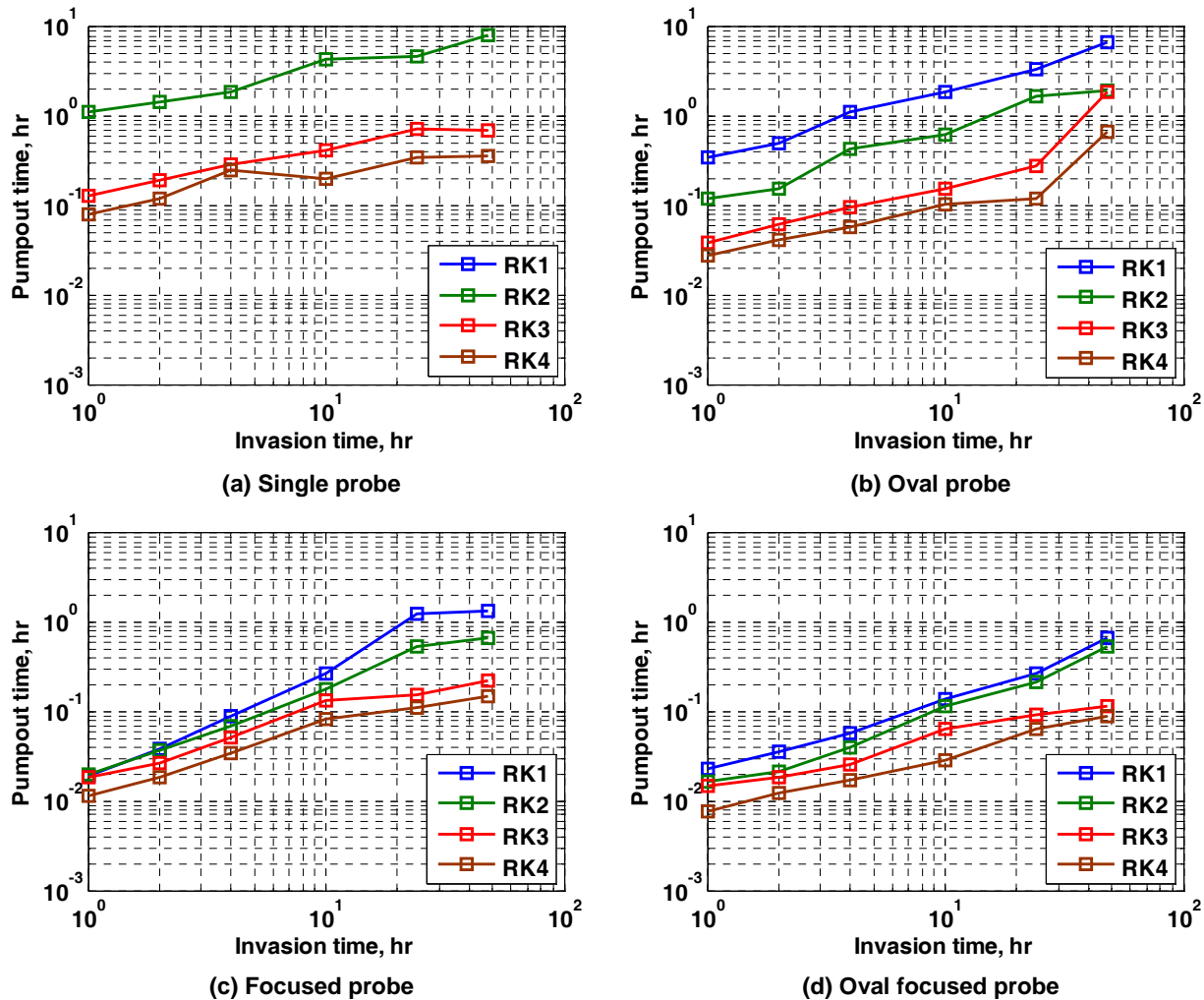


Fig. 12: Assessment of probe behavior for various rock types. The pumpout time necessary to achieve 10% contamination decreases as the permeability and porosity of rock types increase from rock type no. 1 to rock type no. 4. Oval focused probe exhibits the fastest cleanup time for all rock types.

side of the wellbore, pressure drop during pumpout is less than when the probe faces to top of the wellbore. This enables the side facing probe to pump faster, which further reduces the pumpout time.

PROBE BEHAVIOR FOR DIFFERENT ROCK TYPES

Fig. 12 shows the behavior of the probe in four types of rocks. From the pressure drop point of view, the oval probe and oval focused probe impose a lower pressure drop than the single probe and focused sampling probe during fluid pumpout.

The radius of mud-filtrate invasion changes with the rock type. Although the mud has constant properties, the rock type affects the volume of mud invasion. This is demonstrated by the behavior of the probes in the four rock types used. The pump performance curve, described earlier, determines the flow rate of the

pumpout test in each rock type. It also yields the pressure drop of each probe in various reservoirs. Simulation for rock type 1 shows that the single probe cannot achieve 5% contamination. As the permeability and porosity of rocks increase, the probes can achieve a faster cleanup time than in poorer quality rocks.

PROBE BEHAVIOR IN OBM

The same numerical method is used to simulate the case of OBM invading an oil-bearing formation, which results in miscible contamination. The reservoir model changes from black-oil simulator to a compositional Equation-Of-State (EOS) simulator. In this study, in-situ reservoir fluid and OBM filtrate is tracked using Peng-Robinson’s EOS, (Peng and Robinson, 1978). Fluid viscosities are calculated using Lohrenz-Bray-Clark’s (LBC) correlation, (Lohrenz et al., 1964), and fluid phase densities are obtained from the EOS.

TABLE 6: Equation-Of-State parameters and mole fractions of the assumed in-situ hydrocarbon pseudo components

Parameter	N ₂ C ₁	CO ₂ C ₃	C ₄ C ₆	C ₇ C ₁₈	C ₁₉₊
Molar Concent.	0.618	0.079	0.087	0.179	0.036
Critical Temp. (°F)	-126	125.9	359.8	656.2	1060
Critical Press. (psi)	653.3	839.4	498.2	322.3	184.4
Acentric Factor	0.011	0.146	0.230	0.490	0.919
Molecular Weight (lbs/mole)	16.6	36.23	67.73	132.8	303.2
Volume Shift Parameter	-0.19	-0.131	-0.056	0.171	0.231

TABLE 7: Equation-Of-State parameters and mole fractions assumed for the mud-filtrate pseudo components

Parameter	MC ₁₄	MC ₁₆	MC ₁₈
Molar Concentration	0.6489	0.2145	0.1364
Critical Temperature (°F)	755.1	822.5	878.1
Critical Pressure (psi)	261.8	240.2	224.4
Acentric Factor	0.6257	0.7118	0.7842
Molecular Weight (lbs/mole)	190	222	251
Volume Shift Parameter	0.0792	0.0666	0.0439

Table 6 and Table 7 demonstrate the in-situ oil and OBM properties, and the mole fraction of their components. OBM is heavy, dead oil, and in-situ oil is light oil with a significant amount of soluble gas. OBM filtrate invades the formation with the same volume of filtrate loss as that of WBM. However, because of capillary pressure, WBM has a smoother radial front than OBM. **Fig. 14** shows the differences in the contamination front with water and OBM invasion at increasing radial distances from the wellbore.

For the base-case model, rock type 3, with irreducible water saturation, it takes longer for OBM to clean up and reach 10% of contamination than with WBM, however, OBM contamination cleans up faster than WBM at the beginning of the pumpout test. As shown in **Fig. 13**, OBM reaches 80% contamination faster than WBM.

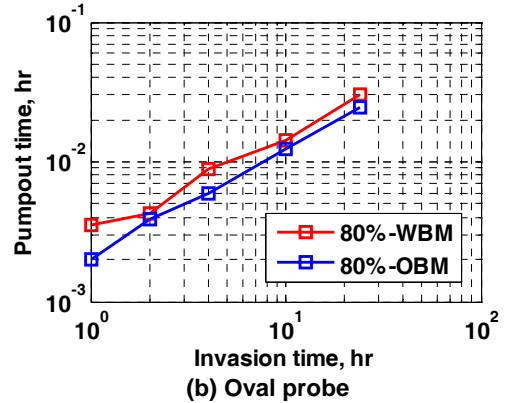
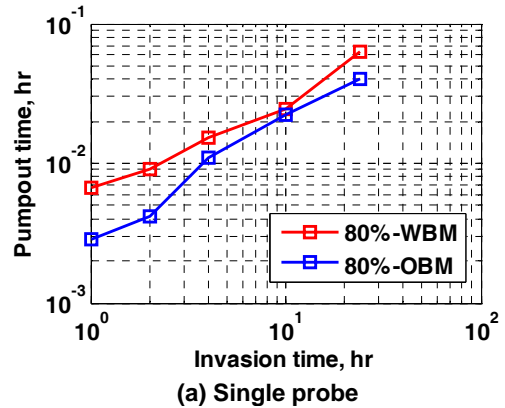


Fig. 13: Comparison of OBM and WBM invasion and fluid sampling effects at an early stage of drawdown when the probes reach 80% of fluid contamination. Results indicate that probes reach 80% of fluid contamination faster in the case of OBM than in the case of WBM.

Because WBM and OBM have the same viscosity, which is higher than the in-situ reservoir oil, both create an invaded zone with a lower mobility than the uncontaminated regions. However, WBM invasion is immiscible, which results in a much lower invaded zone mobility than with OBM. For WBM, the contaminated region is governed by immiscible mixing, which further reduces mobility in the contaminated region as a result of relative permeability effects.

During pumpout, a channel forms to funnel the in-situ oil to the probe. Because of the lower viscosity of native oil, the channel has a lower mobility than the invaded region. With WBM, the formation of this channel is slower because of the reduced mobility of the invaded region, as compared to the OBM. Therefore, after the start of the pumpout test, in the case of OBM, probes withdraw contamination and create a channel more quickly than with WBM.

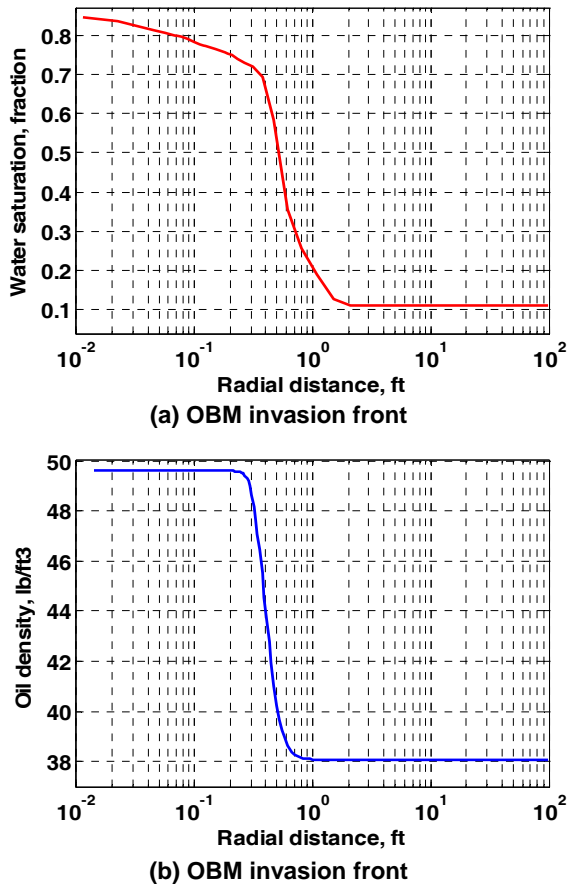


Fig. 14: Simulated radial distributions of water saturation and oil density for the cases of invasion with (a) WBM, and (b) OBM for the base-case model. OBM is miscible with in-situ oil, and nearly exhibits a shock radial concentration front. WBM is immiscible and, because of capillary pressure, exhibits a smoother radial saturation front than the case of OBM-filtrate invasion.

However, as pumpout continues, a more focused channel is formed because the lower mobility WBM invasion region acts as a guard to the oil that has penetrated a path to the probe. This path or channel has a higher mobility because of the reduced contamination (i.e., lower water saturation) than the surrounding WBM invaded region. In the OBM case, the channel formed also has a lower mobility than the surrounding invaded region, but the contrast is much lower. Consequently, OBM filtrate is more mobile and mixes more freely with the oil in the flow channel path to the probe, thereby resulting in a slower cleanup time for the WBM case. This conclusion is best shown in **Fig. 13** and **Fig. 15**, which compare the pumpout time for the

single probe and the oval probe using the base case WBM and OBM models. Both simulation results assume the same radius of mud-filtrate invasion shown in **Fig. 14**.

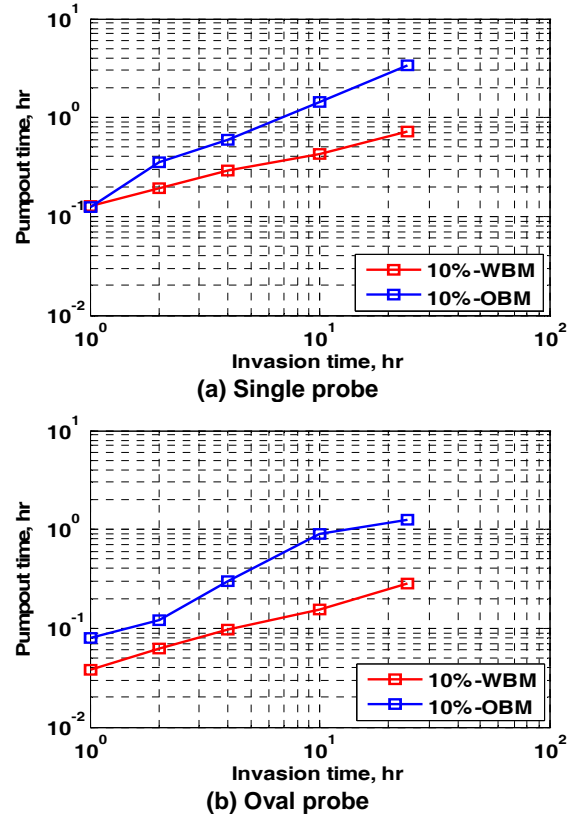


Fig. 15: Invasion time vs. pumpout time necessary to reach 10% of contamination. For the single probe at short invasion times, there are no significant differences between fluid cleanup times for WBM and OBM contamination. However, at long invasion times (wireline formation tester), significant differences arise between WBM and OBM contamination for the single probe. The oval probe achieves a faster cleanup time than the single probe; OBM cleans up more slowly than WBM in this case. Results also show that the probes reach 10% contamination faster in the case of WBM than in the case of OBM.

Fig. 16 illustrates this invaded flow channel pattern by showing the concentration contrast in the flow channel at the beginning and end of a pumpout test. The region surrounding the channel behaves as a non-ideal insulator, and this insulator performs better with WBM than with OBM. The end result is lower contamination leaks into the channel with WBM than OBM and ultimately shorter sampling times with WBM.

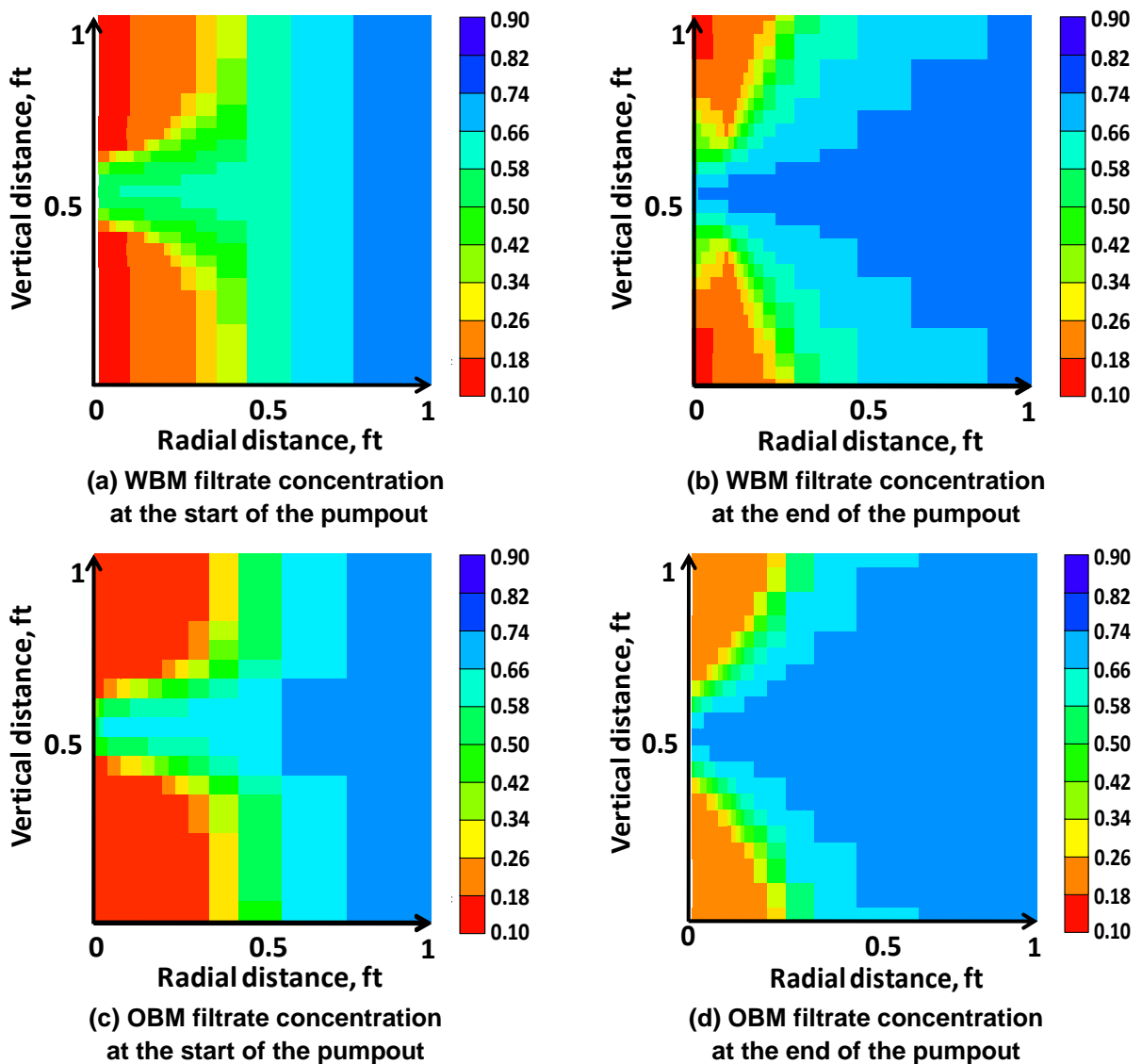


Fig. 16: Comparison of the spatial distribution of WBM and OBM filtrate contamination. The color bar describes the amount of oil concentration. At beginning of the pumpout, higher concentrations of oil enter the probe for the OBM case for WBM. However, at the end of the pumpout, the WBM exhibits higher contamination than OBM at the probe inlet. Therefore, testers operating in the presence of WBM should obtain a clean fluid sample faster than for the OBM case.

OBM CONTAMINATION FUNCTIONS

Estimating the contamination with a miscible mud filtrate poses some difficulties because the filtrate and in-situ oil (or water) can have similar properties. There are currently several methods of estimating contamination used to evaluate the pumpout time for OBM. These contamination functions are based on volumetric measurements of contamination, such as gas-oil ratio (GOR), or molar based measurements, including fluid density and viscosity.

Because GOR is normally measured at the surface, a downhole measurement of GOR would not be a direct measurement and would be subject to correlation errors.

The correlation errors can result in discrepancies in the GOR downhole estimate when compared with the surface measurement. Downhole GOR can also be misleading if gas is produced while sampling because the sampling vessel may not retain both phases effectively. Also, GOR is not directly related to the volume fraction of the contamination.

Austad and Isom (2001) introduced the GOR-based contamination function given by

$$C(t) = 1 - \frac{1}{\frac{\rho_m}{\rho_o} \left\{ \frac{GOR_o}{GOR(t)} - 1 \right\} + 1}, \quad (3)$$

where $C(t)$ is contamination as a function of sampling time, t is time, ρ_m is mud density, ρ_o is in-situ oil density, GOR_o is uncontaminated formation GOR , and $GOR(t)$ is measured GOR .

The corresponding contamination function based on density is given by

$$C(t) = \frac{\rho(t) - \rho_o}{\rho_m - \rho_o}, \quad (4)$$

where $\rho(t)$ is measured density, ρ_o is formation oil density, and ρ_m is mud density.

For the case of viscosity, the contamination function is given by

$$C(t) = \frac{\mu(t) - \mu_o}{\mu_m - \mu_o}, \quad (5)$$

where $\mu(t)$ is measured viscosity, μ_o is formation oil viscosity, and μ_m is mud viscosity. This contamination function assumes that viscosity mixing is linear. However, this function can be modified for non-linear mixing rules, such as Todd and Longstaff's (1972) or the Modified Arrhenius model (Lederer, 1933).

As shown in **Fig. 17**, the GOR contamination estimate always indicates a higher level of contamination than molar-based contamination functions. The density function should be the most accurate because density mixes linearly and the exact densities in the simulations are known *a priori*. However, in practice, when the filtrate and formation fluid densities are similar, the accuracy decreases.

Based on the density contamination function, the cleanup time is calculated for OBM in the base-case model and for the four types of probes shown in **Fig. 18**. For the cases of the focused sampling probe, and the oval focused probe results have the same behavior as that of the single and oval probe respectively, because the shapes of these probes are similar to the each other (i.e., the single and focused sampling probes are circular, and the oval and oval focused probes are elongated). For the case of the single probe, the difference in cleanup time between OBM and WBM becomes significant when invasion times are large, which occurs with wireline formation-testers. For the oval probe, a difference exists between cleanup time for small and large invasion times. As indicated in **Fig. 18**, the oval probe cleans up faster than the single probe in

OBM and WBM cases. For the single probe and focused sampling probe, there is little difference between cleanup times for OBM and WBM when the invasion times are short (i.e., 1 to 2 hours). As **Fig. 18** shows for low invasion times, the oval type probes clean up faster in WBM. In the OBM base case, the single probe requires significantly longer cleanup times than the remaining probes.

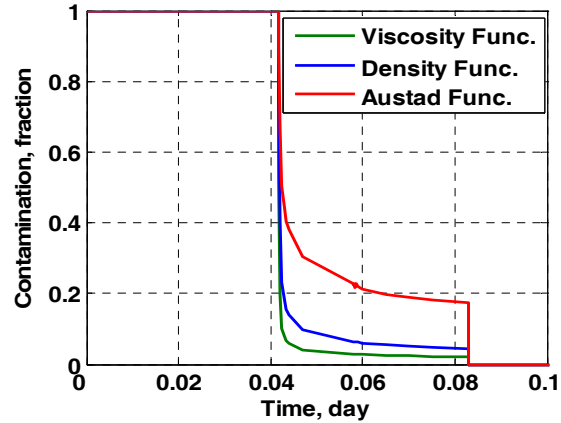
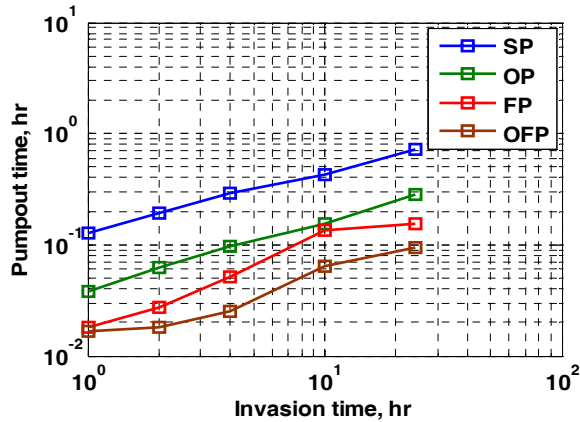


Fig. 17: Three different contamination functions as shown using the base case OBM model. The fluid pumpout test begins after 1 hour of mud-filtrate invasion. The GOR contamination function exhibits a higher level of contamination than the density and viscosity contamination functions. There is no indication of decreasing values of contamination with the GOR function, even as the pumpout time increases.

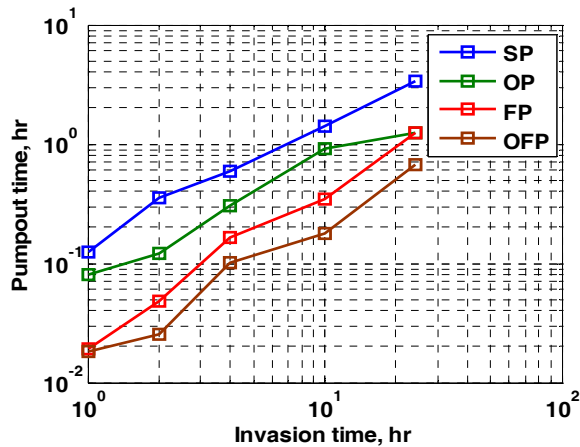
DISCUSSION

A notable improvement with respect to previous related studies is the explicit consideration of dynamic mud-filtrate invasion during fluid pumpout. This was a feature of the simulations because one of the primary goals was to compare wireline testers to while-drilling testers. This study shows that formation testers can secure clean fluid samples soon after drilling much faster than wireline testers in the same conditions. Each probe investigated has its own performance curve and, by considering the available pump and sampling constraints (i.e., saturation pressure), the appropriate probe for a specific rock type can be chosen. Changes in the mobility near the probe are considered because the near wellbore mobility changes affect the pressure drop and are important considerations to pumpout control. The density contamination function is based on a molar-based measurement of contamination, and provides an improved estimate of contamination over the GOR contamination estimates. Although the GOR method is considered to be a volume-based estimate, this method gives a consistently higher contamination

level, compared to the value that can be determined directly from the simulations.



(a) WBM-filtrate invasion



(b) OBM-filtrate invasion

Fig. 18: Efficiency of various probe-type formation-testers in the presence of (a) WBM-filtrate invasion, and (b) OBM-filtrate invasion (OFP = oval focused probe, FP = focused probe, OP = oval probe, SP = single probe). In the case of WBM-filtrate invasion, probes secure a clean fluid sample faster than in the case of OBM-filtrate invasion. Simulations were performed for the base-case model, assuming a reservoir at irreducible water saturation.

When comparing the OBM and WBM simulations, the OBM models clean up faster than WBM at the early time of the pumpout test. However, for testers to acquire low level contamination samples (i.e., less than 10%), a WBM system is normally faster than OBM, regardless of the probe design (see **Fig. 18**).

CONCLUSIONS

The following conclusions stem from the numerical simulations and interpretation studies considered in this paper:

1. While-drilling formation-testers typically have shorter pumpout times than wireline formation testers, even when considering more active invasion while sampling.
2. Based on simulations of different probe designs in a variety of reservoir conditions, the oval focused probe retrieves the cleanest fluid sample in the shortest time, followed by the standard focused probe, the oval probe, and, finally, by the single probe.
3. The largest pressure drop during fluid pumpout corresponds to the single probe, followed by the oval probe, focused sampling probe, and, finally, the oval focused probe.
4. Pumpout cleanup time increases with wellbore deviation angle, regardless of probe type. The effect of wellbore deviation on increasing the cleanup time is the largest for the single probe, followed by the oval probe, focused sampling probe, and the oval focused probe.
5. The pressure drop during pumpout increases with wellbore deviation angle. This behavior may lead to abnormal two-phase flow in the near-borehole region.
6. At irreducible water-saturation conditions and for the same invasion radius, cleanup times are faster for WBM-filtrate invasion than OBM-filtrate invasion.
7. Molar-based contamination functions are more reliable and accurate than volumetric functions, such as GOR, to measure the time evolution of the fluid cleanup.
8. Because of formation anisotropy, capillary pressure, fluid density contrast, and wellbore deviation angle, it is recommended that probes face the upper side of the wellbore when operating in a horizontal well to achieve the shortest fluid cleanup time and to operate at the lowest possible pressure drop during pumpout.
9. Fluid pumpout time increases with decreasing quality of the petrophysical properties (i.e., lower permeability, lower porosity, and higher capillary pressure). For the simulation cases considered, the oval focused or focused sampling probes consistently achieved the fastest cleanup times.

NOMENCLATURE

λ	: Growth factor
$C(t)$: Contamination by time variation
ΔP	: Pressure drop across the mudcake, [psi]
$x_{mc}(t)$: Mudcake thickness, [in]
k_{mc}	: Mudcake permeability, [mD]
$q(t)$: Mud invasion flow rate, [cm ³ /sec/cm ²]
ρ_m	: Mud density, [lb/ft ³]
ρ_o	: In-situ oil density, [lb/ft ³]
μ_m	: Mud viscosity, [cp]
μ_o	: Formation oil viscosity, [cp]

ϕ	: Porosity
k	: Formation permeability, [mD]
k_{ro}	: Oil relative permeability
k_{rw}	: Water relative permeability
GOR	: Gas-oil ratio, [ft ³ /STB]
GOR_o	: Uncontaminated formation GOR, [ft ³ /STB]
$GOR(t)$: Measured GOR, [ft ³ /STB]
OFP	: Oval focused probe
FP	: Focused sampling probe
OP	: Oval probe
SP	: Single probe
S_{wirr}	: Irreducible water saturation
OBM	: Oil-base mud
WBM	: Water-base mud
EOS	: Equation-of-state
FTWD	: Formation-tester while-drilling
LWD	: Logging-while-drilling

ACKNOWLEDGEMENTS

The authors wish to thank Halliburton Energy Services for permission to publish this project and for their funding through a summer internship position offered to Abdolhamid Hadibeik in 2008. The work described in this paper was partially funded by The University of Texas at Austin Research Consortium on Formation Evaluation, jointly sponsored by Anadarko, Aramco, Baker-Hughes, BG, BHP Billiton, BP, Chevron, ConocoPhillips, ENI, ExxonMobil, Halliburton, Hess, Marathon, Mexican Institute for Petroleum, Nexen, Petrobras, Schlumberger, StatoilHydro, TOTAL, and Weatherford. A special note of gratitude goes to Mike Bittar and Bob Engelman (Halliburton Energy Services) for their technical support.

REFERENCES

Alpak, O.F., Elshahawi, H., Hashem, M., and Mullins, O., 2008, Compositional Modeling of Oil-Based-Mud-Filtrate Cleanup during Wireline Formation Tester Sampling: *SPE Reservoir Evaluation and Engineering*, v. 11, no. 2, April, p. 219-232.

Angeles, R., Torres-Verdín, C., and Malik, M., 2009, Predication of Formation-Tester Fluid-Sample Quality in Highly-Deviated Wells: *Petrophysics*, v. 50, no. 1, February, p. 32-48.

Austad, T. and Isom, T.P., 2001, Compositional and PVT Properties of Reservoir Fluids Contaminated by Drilling Fluid Filtrate: *Petroleum Science and Engineering*, v. 30, p. 213-244.

Chin, W.C., 1995, *Formation Invasion, with Applications to Measurement While Drilling, Time Lapse Analysis and Formation Damage*: Gulf Publishing Company, Houston, Texas, p. 28-54, 93-98.

El Zefzaf, T., El Fattah, M.A., Proett, M., Engelman, B., and Bassiouny, A., 2006, Formation Testing and Sampling Using an Oval Pad in Al Hamed Field, Egypt: paper SPE 102366 presented at the SPE Annual Technical Conference and Exhibition, San Antonio, Texas, September 24-27.

Fisk, J.V. and Jamison, D.E., 1989, Physical Properties of Drilling Fluids at High Temperature and Pressures: *SPE Drilling Engineering*, v.4, no. 4, December, p.341-346.

Lederer, E. L., 1933, Proc. World Pet. Cong., v.2, p. 526-28.

Lohrenz, J., Bray, B.G., and Clark, C.R., 1964, Calculating Viscosity of Reservoir Fluids from Their Compositions: *Petroleum Technology Journal*, paper SPE 915, October issue, p. 1171-1176.

Malik, M., Torres-Verdín, C., and Sepehrmoori, K., 2009, A Dual-Grid Automatic History Matching Technique with Applications to 3D Formation Testing in the Presence of Oil-Base Mud: *SPE Journal*, v. 14, no. 1, March, p. 164-181.

Mullins, O.C. and Schroer, J., 2000, Real-Time Determination of Filtrate Contamination During Openhole Wireline Sampling by Optical Spectroscopy: paper SPE 63071 presented at the SPE Annual Technical Conference and Exhibition, Dallas, Texas, October 1-4.

Peng, D.Y. and Robinson, D.B., 1976, A New Two-Constant Equation-Of-State, *Industrial and Engineering Chemistry Fundamentals Journal*, v. 15, no. 59, p. 59-64.

Proett, M., Walker, M., Welshans, D., and Gray, C., 2003, Formation Testing While Drilling, A New Era in Formation Testing: paper SPE 84087 presented at the SPE Annual Technical Conference and Exhibition, Denver, Colorado, October 5-8.

Sherwood, J.D, 2005, Optimal Probes for Withdrawal of Uncontaminated Fluid Samples, *Physics of fluids*, v. 17, issue 8, p. 083102-083102-10.

Todd, M.R. and Longstaff, W.J., 1972, The Development, Testing and Application of a Numerical Simulator for Predicting Miscible Flood Performance, *Journal of Petroleum Technology* (July), p. 874-77.

Wu, J., Torres-Verdín, C., Sepehrmoori, K., and Delshad, M., 2004, Numerical Simulation of Mud-Filtrate Invasion in Deviated Wells, *SPE Reservoir Evaluation and Engineering*, v.7, no. 2, April, p.143-154.